Conf-911133--4

DESIGN OF ZEOLITE ION-EXCHANGE COLUMNS FOR WASTEWATER TREATMENT

CONF-911133--4

DE92 001959

S. M. Robinson*, W. D. Arnold, and C. H. Byers

Oak Ridge National Laboratory†
Oak Ridge, Tennessee 37831

Prepared for presentation at
American Institute of Chemical Engineers 1991 Annual Meeting
Los Angeles, CA, November 17-22, 1991
Session 69: Design of Adsorption Systems

*Author to whom correspondence is to be addressed

†Managed for the U.S. Department of Energy by Martin Marietta Energy Systems, Inc., under contract DE-AC05-84OR21400

DESIGN OF ZEOLITE ION-EXCHANGE COLUMNS FOR WASTEWATER TREATMENT

S. M. Robinson, W. D. Arnold, and C. H. Byers

Oak Ridge National Laboratory
Oak Ridge, Tennessee 37831

Oak Ridge National Laboratory plans to use chabazite zeolites for decontamination of wastewater containing parts-per-billion levels of ^{90}Sr and ^{137}Cs. Treatability studies indicate that such zeolites can remove trace amounts of ^{90}Sr and ^{137}Cs from wastewater containing high concentrations of calcium and magnesium. These studies show that zeolite system efficiency is dependent on column design and operating conditions. Previous results with bench-scale, pilot-scale, and near-full-scale columns indicate that optimized design of full-scale columns could reduce the volume of spent solids generation by one-half. The data indicate that shortcut scale-up methods cannot be used to design columns to minimize secondary waste generation. Since the secondary waste generation rate is a primary influence on process cost effectiveness, a predictive mathematical model for column design is being developed. Equilibrium models and mass-transfer mechanisms are being experimentally determined for isothermal multicomponent ion exchange (Ca, Mg, Na, Cs, and Sr). Mathematical models of these data to determine the breakthrough curves for different column configurations and operating conditions will be used to optimize the final design of a full-scale treatment plant.

INTRODUCTION

Fixed-bed ion exchange in which resins serve as the granular medium has been established for many years as an important technique for water purification and the recovery of ionic components from mixtures. Inorganic media, such as porous, crystalline, aluminosilicate zeolites, have had limited application as ion exchangers in the past. However, zeolite molecular sieves have several characteristics that are unique compared to ion-exchange resins. They are porous crystalline aluminosilicates with rigid frameworks with

open crystal lattice containing pores of precisely uniform molecular dimensions with no distribution of pore size. Therefore, zeolites exhibit both molecular-sieve and ion-exchange properties. They also tend to be cheaper than many organic resins and are resistant to thermal and radiation degradation. As the field of applications for ion exchange broadens, a class of applications has developed where economic considerations, a high thermal and/or radiation flux, or the molecular sieve properties of zeolites make them more attractive than ion-exchange resins (*1*).

Some of these considerations have led Oak Ridge National Laboratory (ORNL) to use chabazite zeolites for decontamination of process wastewater containing parts-per-billion levels of ^{90}Sr and ^{137}Cs. The wastewater *(2,3)* typically contains 4000 Bq/L of ^{90}Sr and 400 Bq/L of ^{137}Cs. The discharge limits are 37 and 111 Bq/L, respectively. The concentrations of other radionuclides are well below discharge limits. The pH of the wastewater is typically 8.8, and it contains 250 mg/L total dissolved solids, 3 mg/L total suspended solids, 133 mg/L total hardness, 125 mg/L alkalinity, and 12 mg/L total organic carbon. The major chemical constituents are bicarbonates of calcium, magnesium, and sodium.

Treatability studies (*2, 3*) indicate that chabazite zeolites are highly selective for cesium and strontium while admitting high loadings of calcium and magnesium. Thus, they are suited to the removal of trace amounts of ^{137}Cs and ^{90}Sr from ORNL wastewaters. These studies also indicate that the efficiency of the zeolite system depends strongly on the column design and operating conditions and that through optimization of the design of full-scale columns, one could halve the generation rate of loaded zeolite requiring disposal. The design of zeolite systems for minimization of secondary waste is a key to economic operation of the zeolite ion-exchange plant for treatment of radioactive waste.

The objective of this paper is to present experimental ion-exchange data for synthetic mixtures that simulate ORNL's process wastewater. Experimental equilibrium and mass-transfer data will be compared with available predictive models to assess the most appropriate model for the ion-exchange systems relevant to the problem at hand.

BACKGROUND

Although fixed-bed ion exchange has been an important unit operation for purification and component recovery for many years, the analysis of its application to this process is complex. Ion exchange in a fixed-bed column is characterized by a breakthrough curve that is the effluent concentration profile as a function of the volume of liquid processed. The rate of appearance and the shape of breakthrough profiles depend on several factors, including the physical and chemical properties of the sorbate and sorbent, the equilibrium relationship between the solution and solid phases, the rate limiting mass-transfer mechanisms (film diffusion, particle diffusion, pore diffusion, axial dispersion, or reaction kinetics), the bed depth, and the fluid velocity. The objective of fixed-bed column design is to predict the characteristics of the breakthrough curve for a particular column operating under a given set of conditions.

Models of multicomponent liquid ion-exchange systems were virtually nonexistent before the 1980s. Although a considerable effort has been made in this area, multicomponent models have not been developed to the point where they can be used in general industrial applications without using laboratory- or pilot-scale data to predict the

equilibrium and mass-transfer relationships (*4, 5*). The decontamination of radioactive waste solutions using zeolites has been studied since the 1950s. Unfortunately, very few fundamental studies have been done, and it has been difficult to make use of much of the literature because of the lack of standardized procedures and theoretical bases (*6*). Predictive modeling for most multicomponent systems is complicated by competitive interactions among species. In the case of microporous materials such as zeolites, these interactions are further complicated by mutual interference in intraparticle mass transport as well as competition for available ion-exchange sites (*7*). Since mathematical models have not been available for column design of such systems, users have been restricted to designing columns based on pilot-plant tests and/or crude models. Neither of these approaches have been very successful for efficient column design.

A predictive mathematical model is being developed for the design optimization of ion-exchange columns containing chabazite zeolites. This project consists of two phases: (1) experimental studies to determine equilibrium equations and mass-transfer coefficients and (2) mathematical modeling to predict breakthrough data for designing full-scale ion-exchange columns. To date, the equilibrium and mass-transfer studies have been performed. The equilibrium studies have been described in detail elsewhere (*8, 9*) and are summarized here.

THEORY

Binary ion exchange in zeolites may be represented by the following chemical reaction equation (*10*):

$$g_A B_{(z)}^{g_B^+} + g_B A_{(s)}^{g_A^+} \rightleftharpoons g_A B_{(s)}^{g_B^+} + g_B A_{(z)}^{g_A^+} , \tag{1}$$

where g_A and g_B are the charges of the exchanging cations A and B, and the subscripts z and s refer to the zeolite and solution phases, respectively. The equivalent fractions of the exchanging cations in the solution and zeolite are defined by

$$A_s = g_A c_A / (g_A c_A + g_B c_B) , \tag{2}$$

and

$$A_z = \frac{\textit{equivalents of exchanging cation A}}{\textit{total equivalents of cations in the zeolite}} , \tag{3}$$

where c_A and c_B are the molalities of the ions A and B, respectively, in the equilibrium solution.

A model that describes the behavior of ion exchange in packed beds must predict the S-shaped breakthrough curve that results from ion-exchange material becoming loaded with the solute. Mass balances performed on each solute in the liquid phase leads to the following relationship (*11*):

$$D_z \frac{\partial^2 c}{\partial z^2} = \upsilon \frac{\partial c}{\partial z} + \frac{\partial c}{\partial t} + \rho \left(\frac{1-\epsilon}{\epsilon} \right) \frac{\partial \bar{q}}{\partial t} . \quad (4)$$

The mass transfer from the liquid phase to the solid phase is modeled by the mass transfer across the liquid film surrounding the ion-exchange particles and equations to predict mass transfer resistance inside the particle. Zeolites have two types of intraparticle mass transfer resistances: macropore diffusion through the porous binder and micropore diffusion through the zeolite crystals. Equations that represent the mass transfer through these three phases are (*11*):

$$\frac{\partial \bar{q}}{\partial t} = \frac{3}{\rho R_p} k_f (c_d - c_p), \quad (5)$$

$$\frac{1}{R_p^2} \frac{\partial}{\partial R_p} \left(R_p^2 D_p \frac{\partial c}{\partial R_p} \right) = \frac{\partial c}{\partial t} + \rho \left(\frac{1-\epsilon_p}{\epsilon_p} \right) \frac{\partial \bar{q_c}}{\partial t} , \quad (6)$$

and

$$\frac{\partial q_c}{\partial t} = \frac{1}{r^2} \frac{\partial}{\partial r} \left(r^2 D_c \frac{\partial q_c}{\partial r} \right) , \quad (7)$$

where k_f, D_p, and D_c are the film, macropore, and micropore mass-transfer coefficients, respectively. Equations 4 through 7 are coupled with an equilibrium equation and solved by numerical methods to predict ion-exchange breakthrough curves.

The majority of the models currently used for wastewater treatment systems are phenomenological since multicomponent interactions are incorporated implicitly into the model coefficients. Equilibrium equation coefficients and the film mass-transfer coefficient

are often estimated using semi-empirical correlations. Effective intraparticle diffusion coefficients are determined from experimental data using models that contain the above estimated coefficients. Once the intraparticle diffusion coefficients are found, the model is used to predict breakthrough curves at other conditions. The value of a phenomenological model is directly related to the accuracy of the model input parameters (*4*).

The complexity and diversity of the mechanisms of single and multicomponent ion-exchange equilibrium behavior have led to the development of a large number of equations, both theoretical and empirical in nature. Useful reviews of this area by Soldatov and Bichkova (*12*), Myers and Byington (*13*), and Shallcross et al. (*14*) are available. The most frequently used models are the following:

the binary Langmuir model,

$$q = \frac{q_s bc}{1+bc} = \frac{ac}{1+bc} \; ; \tag{8}$$

the binary Freundlich model,

$$q = kc^n \; ; \tag{9}$$

and the Dubinin-Polyani model,

$$q = q_s \exp\{-kR^2T^2[\ln(\frac{c_m}{c})]^2\} \; . \tag{10}$$

In these equations, q and c are the equilibrium concentrations in the solid and liquid phases, respectively, q_s is the saturation concentration in the solid, and b, n, and k are coefficients fitted to the experimental data.

These models may be extended in a logical manner to describe multicomponent equilibrium. For instance, the multicomponent Langmuir model is

$$\frac{q_i}{q_{si}} = \frac{b_i c_i}{1+b_1 c_1+b_2 c_2+\ldots b_m c_m} , \tag{11}$$

and the multicomponent Freundlich equation is

$$\frac{q_i}{q_{si}} = \frac{b_i c_i^{n_i}}{b_1 c_1^{n_1}+\ldots\ b_m c_m^{n_m}} . \tag{12}$$

The coefficients, b_i and n_i, are obtained from binary isotherm data.

The multicomponent form of the Dubinin-Polyani equation (*11*) for liquids can be written as

$$q = \exp\left\{b_0 + b_1 \cdot ln(c) + b_2 \cdot [ln(c)]^2\right\} , \tag{13}$$

where

$$b_0 = ln(q_s) - kR^2T^2[ln(c_m)]^2 ,$$

$$b_1 = 2kR^2T^2 ln(c_m) ,$$

and

$$b_2 = -kR^2T^2 . \tag{14}$$

The Ideal Adsorbed Solution Theory (IAST) model is based on the Gibbs adsorption equation and only requires single-solute data to predict multicomponent equilibrium. When the binary Freundlich adsorption isotherm equation is substituted into the IAST model, the following equation can be obtained for modeling purposes (*15*):

$$c_i = \frac{q_i}{\sum_{j-1}^{m} q_j} \left(\frac{\sum_{j-1}^{m} \frac{q_j}{n_j}}{\frac{k_j}{n_j}} \right)^{\frac{1}{n_i}} \quad for\ i = 1\ to\ m\ . \tag{15}$$

Intraparticle mass-transfer coefficients are usually calculated by fitting Equations 4 through 7 to experimental data. Although molecular diffusion theory-based, empirical, and semiemperical correlations are available for predicting macropore diffusion coefficients, they tend to be inaccurate for complex liquid mixtures (*11*). As a result, macropore diffusion coefficients tend to be calculated from experimental data. Micropore diffusion coefficients for zeolites must be calculated from experimental data. Since the equations used to predict ion-exchange column behavior contain k_f, the accuracy of estimating the film mass-transfer coefficient has a major impact on the values calculated for the intraparticle mass transfer coefficients and the model effectiveness.

Film mass-transfer coefficients are traditionally determined from correlations available in the literature or from modeling experimental data. If film mass-transfer coefficients are determined from dynamic modeling of ion-exchange column data, the intraparticle diffusion coefficients must also be obtained from the model. In this case, one of two approaches is usually taken to determine the mass-transfer coefficients: (1) the film mass-transfer coefficient is calculated from the initial experimental data when film mass-transfer mechanisms are dominant, or (2) the film and intraparticle mass-transfer coefficients are determined simultaneously using a multicomponent search method. Potential problems exist with each of these methods.

Correlations developed for film mass transfer in columns contain relationships between the dimensionless Reynolds (Re), Schmidt (Sc), and Sherwood (Sh) Numbers. Some of the more widely used correlations are listed below (*4, 11, 16*).

A correlation was developed for packed beds by Williamson, et al., *(17)* for $0.08 < Re < 125$ and $150 < Sc < 1300$:

$$Sh = 2.4 \in Re^{0.34} Sc^{0.42}. \tag{16}$$

Wilson and Geankoplis *(18)* developed a similar correlation for $0.0016 < \epsilon Re < 55$ and $950 < Sc < 70{,}000$,

$$Sh = 1.09 \in^{-2/3} Re^{1/3} Sc^{1/3}. \tag{17}$$

Ohaski, et al., *(19)* developed:

$$Sh = 2+1.58\ Re^{0.4}\ Sc^{1/3}\ for\ 0.001<Re<5.8, \tag{18}$$

$$Sh = 2+1.21\ Re^{0.5}\ Sc^{1/3}\ for\ 5.8<Re<500, \tag{19}$$

and

$$Sh = 2 + 0.59\ Re^{0.6}\ Sc^{1/3}\ for\ Re>500. \tag{20}$$

Gnielinsk *(20)* developed the following correlation for $1<Re<10{,}000$ and $0.6 <Sc<10{,}000$:

$$Sh = \left[2 + \left(Sh_L^2 + Sh_T^2\right)^{0.5}\right]\ [1 + 1.5\ (1-\epsilon)], \tag{21}$$

where

$$Sh_L = 0.644 Re^{1/2} Sc^{1/3},$$

and

$$Sh_T = 0.037 Re^{0.8} Sc / [1 + 2.443 Re^{-0.1} (Sc^{2/3} - 1)] \quad (22)$$

Kataoka, et al., *(21)* developed an equation for

$$Re[\epsilon/(1-\epsilon)] < 100:$$

$$Sh = 1.85[(1-\epsilon)/\epsilon]^{1/3} Re^{1/3} Sc^{1/3}. \quad (23)$$

Dwivedi-Upadhyay *(22)* found that for $0.01 < Re < 15{,}000$,

$$Sh = (1/\epsilon) [0.765(\epsilon Re)^{0.18} + 0.365(\epsilon Re)^{0.614}] Sc^{1/3}. \quad (24)$$

The correlation developed by Ranz and Marshall *(23)*,

$$Sh = 2.0 + 0.6 Sc^{1/3} Re^{1/2}, \quad (25)$$

is based on mass-transfer rates for freely falling solid spheres.

Wakao and Funazkii *(24)* developed

$$Sh = 2.0 + 1.1 Sc^{1/3} Re^{0.6}. \quad (26)$$

by correcting previous correlations for axial dispersion *(11)* for $3 < Re < 10^4$.

Such correlations usually have been obtained experimentally from media that are significantly different from ion-exchange material and do not account for axial dispersion (*4, 11, 25*). A number of studies have demonstrated that the surface topography and roughness of an ion-exchange material as well as column operating conditions that affect axial dispersion can have an impact on the value obtained for the film mass-transfer coefficients.

Furthermore, no standardized criteria have been established for determining which correlation may be best for a given system, except for hydrodynamic conditions. The applicability of such correlations for a given situation must be verified.

In an attempt to improve predictions of mass-transfer coefficients, the microcolumn or short-bed adsorber (SBA) was developed (*4, 25, 26*). The column is designed to be short enough that immediate breakthrough occurs. According to the designers, the initial stage of the breakthrough curve is always dominated by film transfer. Since the initial portion of the SBA breakthrough curve is insensitive to intraparticle mass transfer, the value of k_f can be obtained by solving Equations 4 and 5 assuming D_z, c_p, and dc/dt are zero as t approaches zero. Under these conditions,

$$k_f = -\frac{\upsilon R_p \epsilon}{3L(1-\epsilon)} \ln (c/c_0). \qquad (27)$$

Once the film mass-transfer coefficient has been determined, the intraparticle mass-transfer coefficients can be estimated by fitting the entire breakthrough curve using Equations 4 through 7, plus the equilibrium equation.

Studies are often performed in batch stirred reactors where the stirrer speed can be controlled to minimize the film mass transfer. If the uptake curves are not a function of the stirrer speed, the film mass-transfer coefficient is often assumed to be negligible and the intraparticle diffusion coefficients are calculated from the experimental data. Ruthven (*11*) reports that this is not always valid, particularly when Carberry-type batch reactors are used, and film mass transfer should be accounted for to avoid miscalculating intraparticle mass-transfer coefficients.

Film mass-transfer correlations for batch reactors have been developed using relationships based on the particle-liquid slip velocity (relative velocity between the liquid and particles), the terminal velocity of free falling particles, or the power input from the stirrer. Some of the more widely used correlations for batch reactors are listed below (*27, 28, 29*).

Treybal *(29)* suggests using a correlation based on the stirrer power input:

$$Sh = 2 + 0.47 Re_p^{0.62} (d_i/d_t)^{0.17} Sc^{0.36} \quad (28)$$

Letterman *(27)* suggests using one of two correlations that are based on the Gilliland-Sherwood and Froessling equations, respectively:

$$Sh = 0.77\left[\frac{P(2R_p)^4 \rho_L^3}{\mu^3}\right]^{0.159} Sc^{1/3} \quad (29)$$

and

$$Sh = 2 + 0.64\left[\frac{P(2R_p)^4 \rho_L^3}{\mu^3}\right]^{-.197} Sc^{1/3}. \quad (30)$$

Sherwood, Pigford, and Wilke *(28)* suggest using Equation 25 to calculate k_f where the Reynolds Number is based on the terminal velocity of free falling particles:

$$Re = \frac{G(2R_p)^3 \rho_L |\rho - \rho_L|}{18\mu^2}. \quad (31)$$

Researchers have indicated that film mass transfer dominates the initial uptake rate in batch reactors (*30, 31*). Since the initial portion of the uptake curve is insensitive to

intraparticle mass transfer, it can be modeled using Equations 4 and 5 in a manner similar to the SBA evaluation:

$$k_f = \cdot\cdot(\rho/1-\rho)\,\frac{R_p}{3}\,\frac{\Delta(c/c_0)}{\Delta t}\,\Big|_{t=0}. \qquad (32)$$

This approach to determining k_f is often known as the initial slope method. Once the film mass-transfer coefficient has been determined, the intraparticle mass-transfer coefficients can be estimated by fitting the entire uptake curve.

EXPERIMENTAL

Chabazite zeolite is available both in natural (e.g., Tenneco Specialty Minerals, TSM-300) and synthetic (e.g., Union Carbide Ionsiv IE-90 or IE-96) form. Ionsiv IE-96, a pelletized form of Ionsiv IE-90 crystals in a clay binder, was used as the sorbent in these studies. Structurally, chabazite consists of stacked, double six-membered ring prisms, interconnected through four rings, in a cubic, close-packed array (*10, 11*). Repetition of the stacking of prisms produces 11 x 6.6 Å cylindrical cavities, joined to adjacent cavities through six eight-membered rings with 4.1 x 3.7 Å free diameters. The eight-membered rings have free apertures of 4.3 Å, and six-membered rings have 2.6-Å diameters. The neutralizing cation mainly coordinates to water molecules in the eight-membered rings. It is coordinated only to the oxygen in the double six-membered ring. As a result, the six-membered rings are not usually active in ion-exchange.

The Ionsiv IE-96 was obtained from Union Carbide in the hydrated sodium form as 20- to 50-mesh (840- to 297-μm) irregularly shaped particles. Most of the material is 30 to

35 mesh (590 to 500 μm), and the laboratory measurements were usually made with fractions of this size fraction. Some tests were performed with particles as small as 24 μm. The Ionsiv IE-90 was obtained as 24 μm irregularly shaped particles and was converted to the sodium form before use.

Simulated wastewater solutions were used in the experimental tests to avoid variability in feed composition. The solutions were prepared by dissolving various amounts of $SrCl_2 \bullet 6H_2O$, CsCl, $CaCl_2$, and $MgCl_2 \bullet 6H_2O$ in demineralized water. The solutions containing strontium and cesium were also spiked with ^{85}Sr and ^{137}Cs tracers, respectively. The calcium and magnesium concentrations in the simulated wastewaters were the same as the ORNL process wastewater, but the strontium and cesium concentrations were increased so that residual concentrations in the equilibrated solutions could be accurately measured with available analytical equipment.

The concentrations of cations in the solution phase were measured using the atomic absorption or gamma-counting analytical equipment. The concentrations of cations in the zeolite were calculated from mass balances using the initial and final solution concentrations. All batch tests were performed in triplicate. All tests were performed at room temperature (23 °C).

Equilibrium isotherms were obtained using a batch method in which the solution phase volume was held constant at 10 mL and the solids dosage was varied between 0.002 and 0.4 g. The solution and solids were contacted for 24 h to obtain each isotherm point. The binary isotherms are given in Fig. 1, and multicomponent isotherms are shown in Figs. 1 and 2.

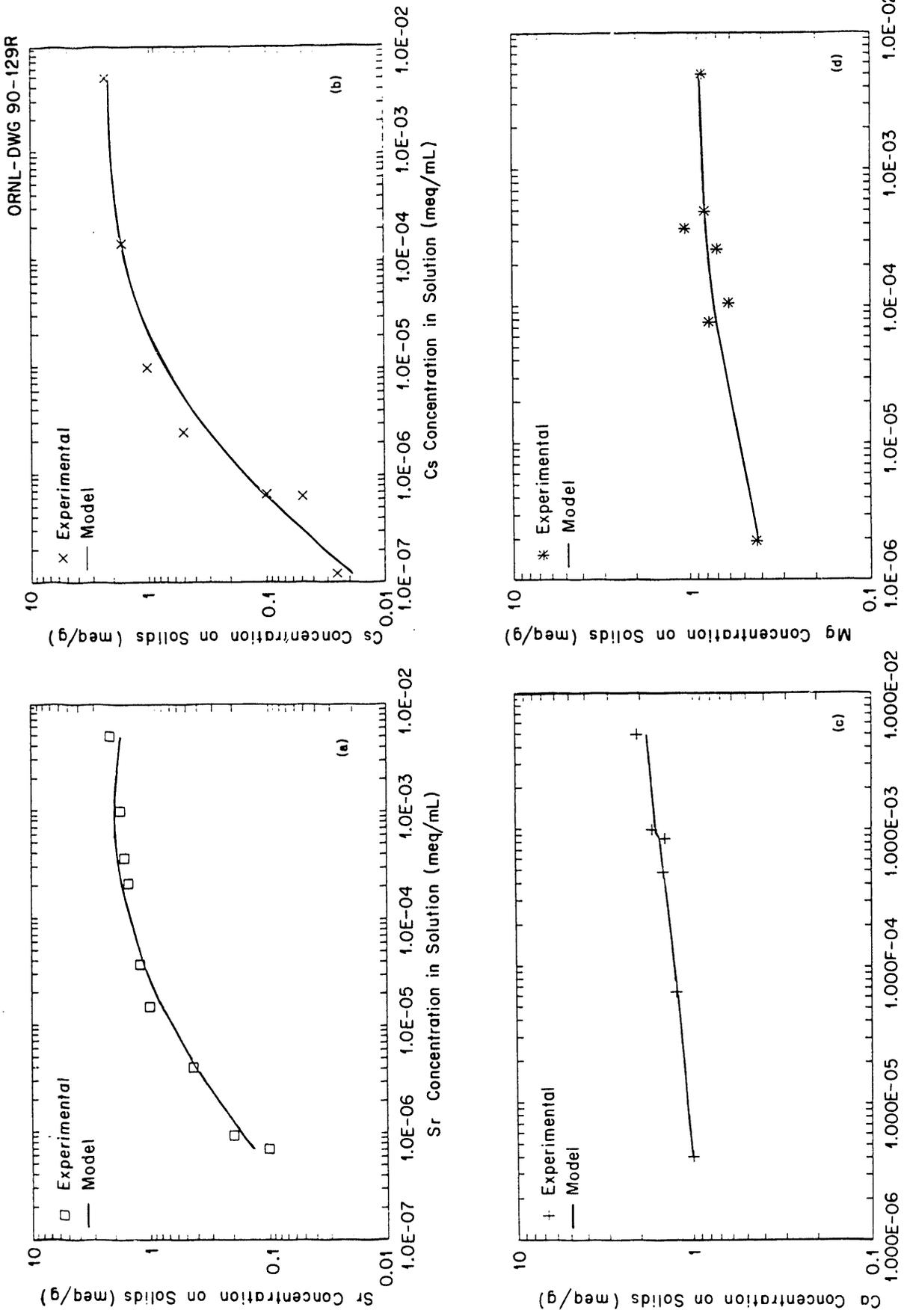

Figure 1. Isotherms for binary ion exchange: (a) Sr-Na (b) Cs-Na (c) Ca-Na (d) Mg-Na. (Reproduced with permission from Ref. 8, 9)

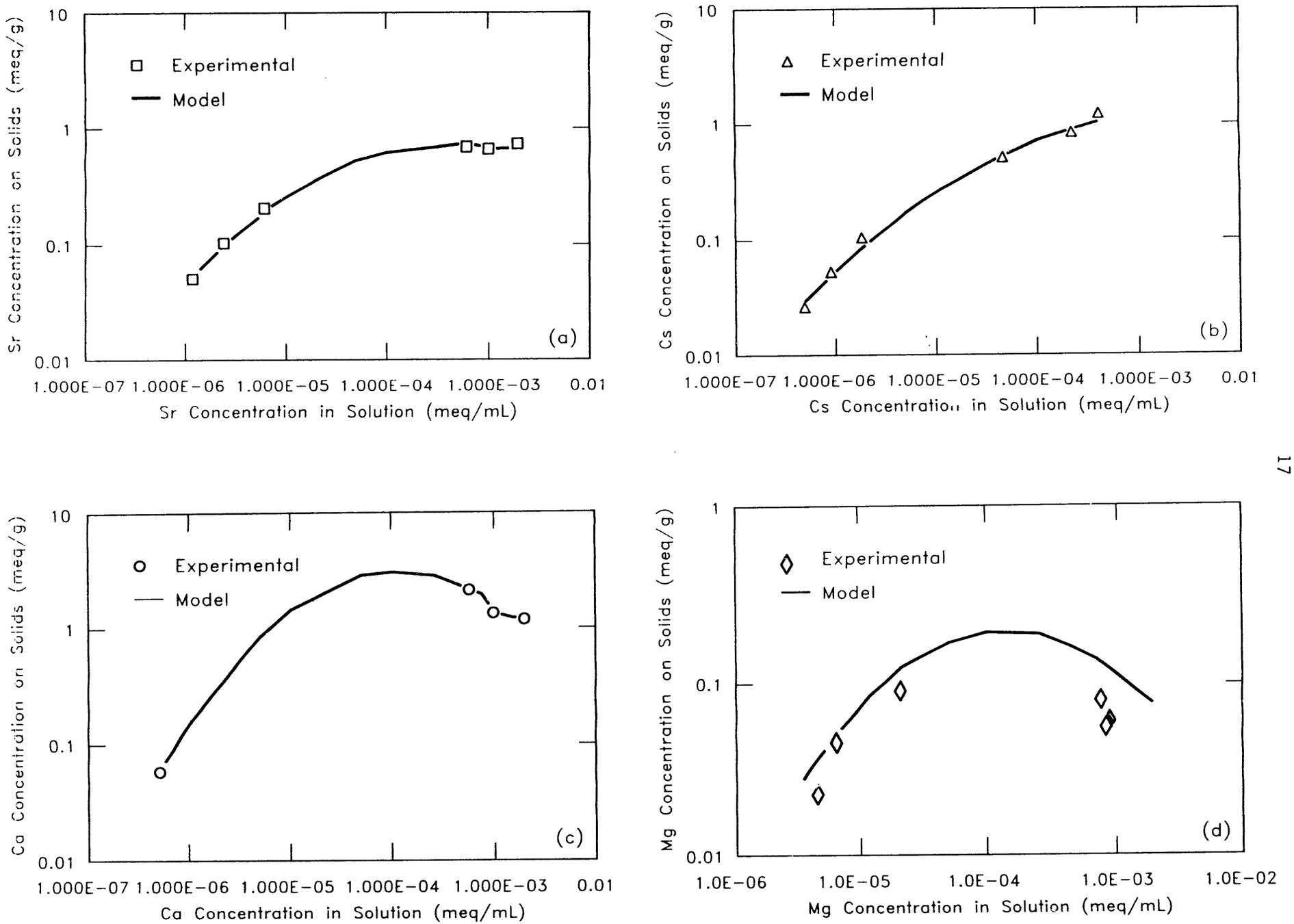

Figure 2. Isotherms for Sr-Cs-Ca-Mg-Na ion-exchange: (a) Sr (b) Cs (c) Ca (d) Mg. (Reproduced with permission from Ref. 8, 9)

Tests to determine mass-transfer coefficients were performed using both a batch reactor and SBA. The SBA is a 1-cm diam column that contains 1 g zeolite Ionsiv IE-96, which results in a bed depth of 1.6 cm. The column was operated with flow rates ranging between 3 and 12 mL/min. Typical breakthrough curves are given in Figs. 3-5.

The batch reactor is a Carberry-type reactor (*11*) that consists of a 5.2-cm diam baffled vessel with a 2.6-cm wide, 1.2-cm high glass impeller. The system was operated with 80 mL of solution and 0.05 g of zeolite (both Ionsiv IE-90 and IE-96 were tested) attached to the impeller in a 100-mesh stainless steel envelope. Impeller speeds varied between 500 and 1000 rpm. Impeller speeds did not impact the uptake rates in these ranges, so most experiments were performed at 750 rpm. Typical uptake curves are shown in Fig. 6.

RESULTS AND DISCUSSION

Standard isotherm equations *(8, 9)* were used to model the equilibria data shown in Figs. 1 and 2. The Langmuir model, the Freundlich model, and the Dubinin-Polyani model, each fit the binary data. The coefficients b_0, b_1, and b_2 for Equation 13 were also determined by numerically fitting the experimental data. This was the best for predicting the data for all four systems. The coefficients obtained for the four cations with this model are given in Table 1. Equation 13 also accurately modeled each of the multicomponent isotherms. These coefficients are also listed in Table 1. The multicomponent isotherms were not accurately predicted by the standard multicomponent Langmuir, Freundlich, Langmuir-Freundlich, Dubinin-Polyani, or the IAST equations.

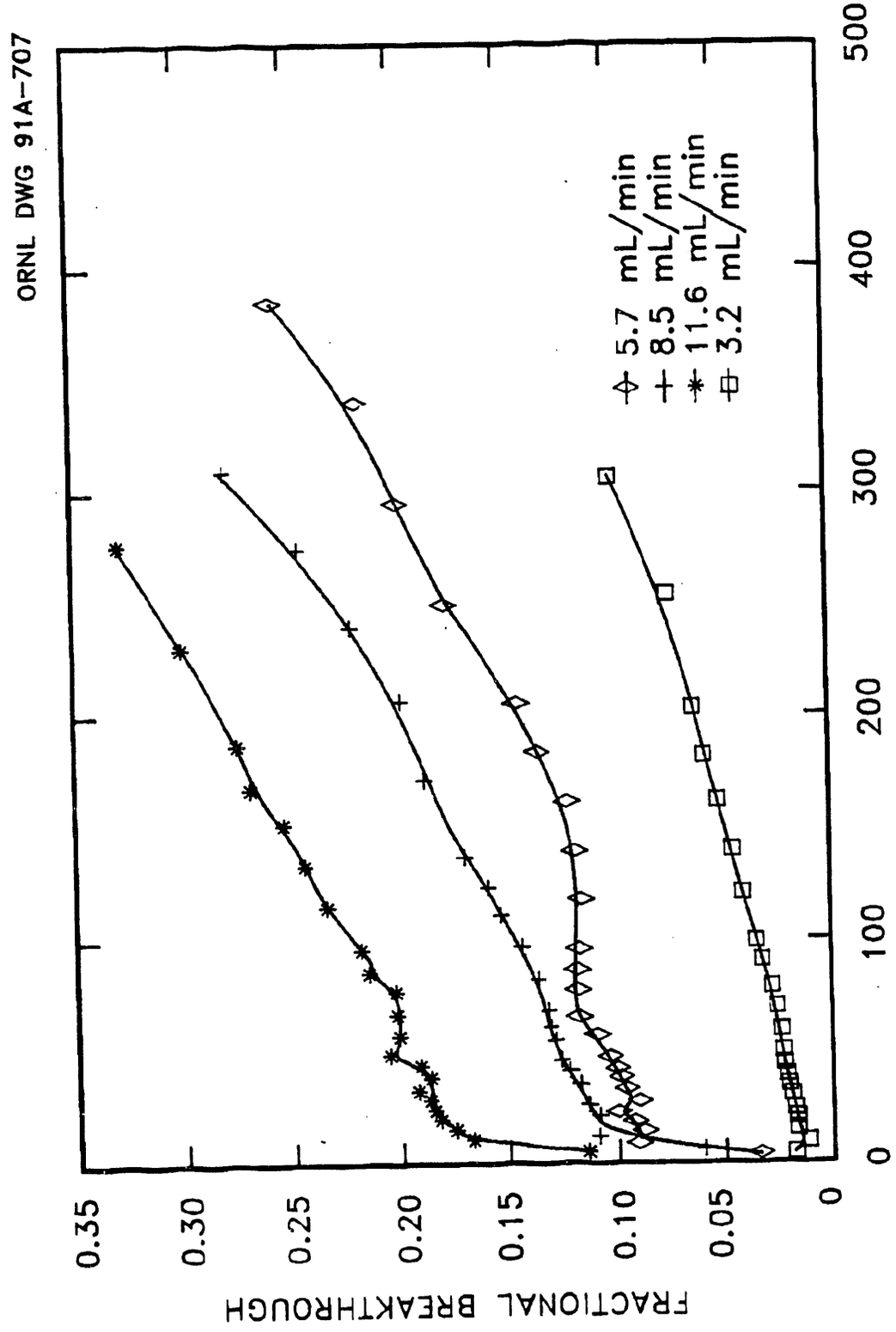

Figure 3. Effect of flow rate on breakthrough curves for short-bed adsorber with $CaCl_2$ feed.

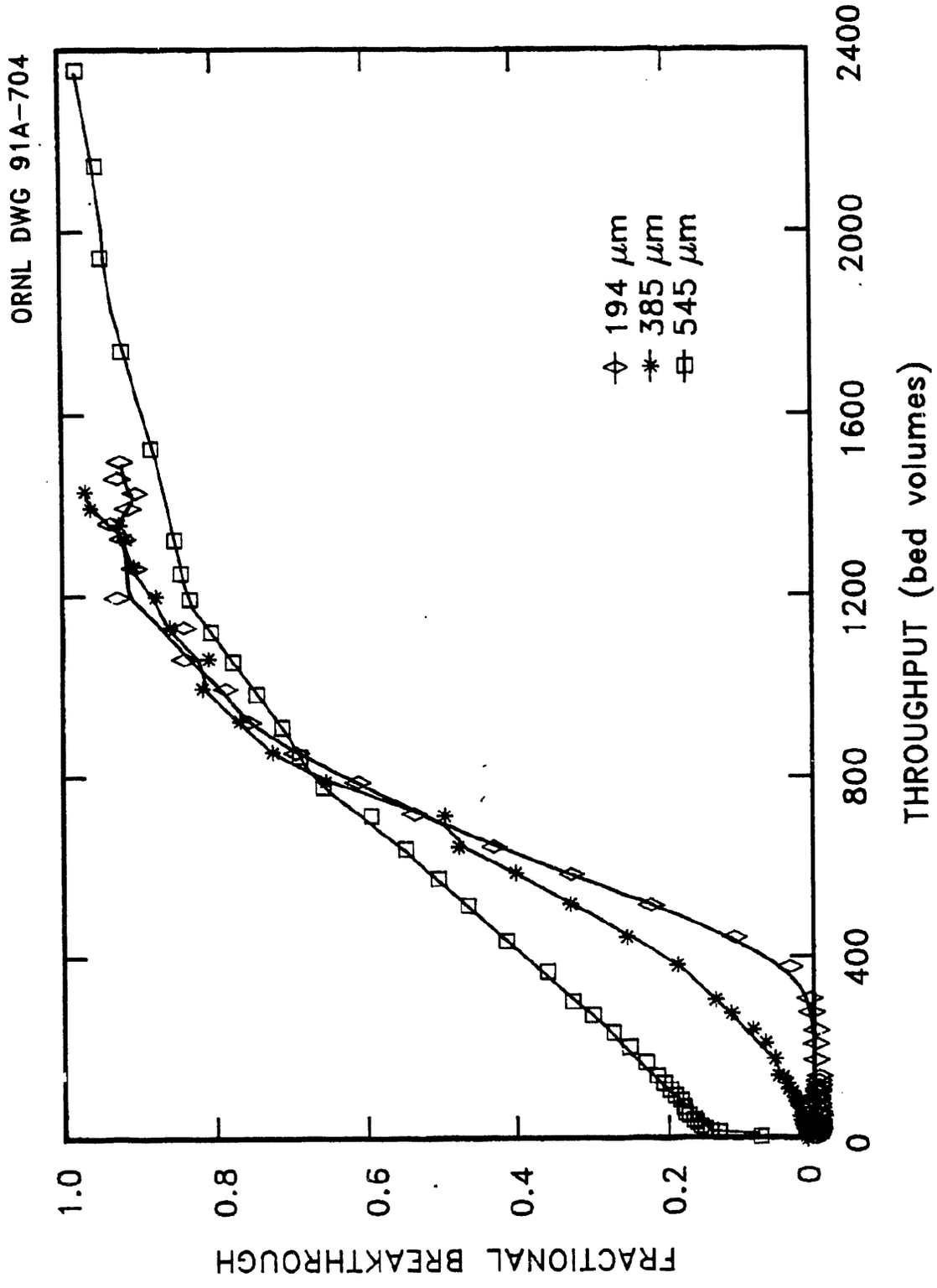

Figure 4. Effect of particle size on breakthrough curves for short-bed adsorber with CaCl feed.

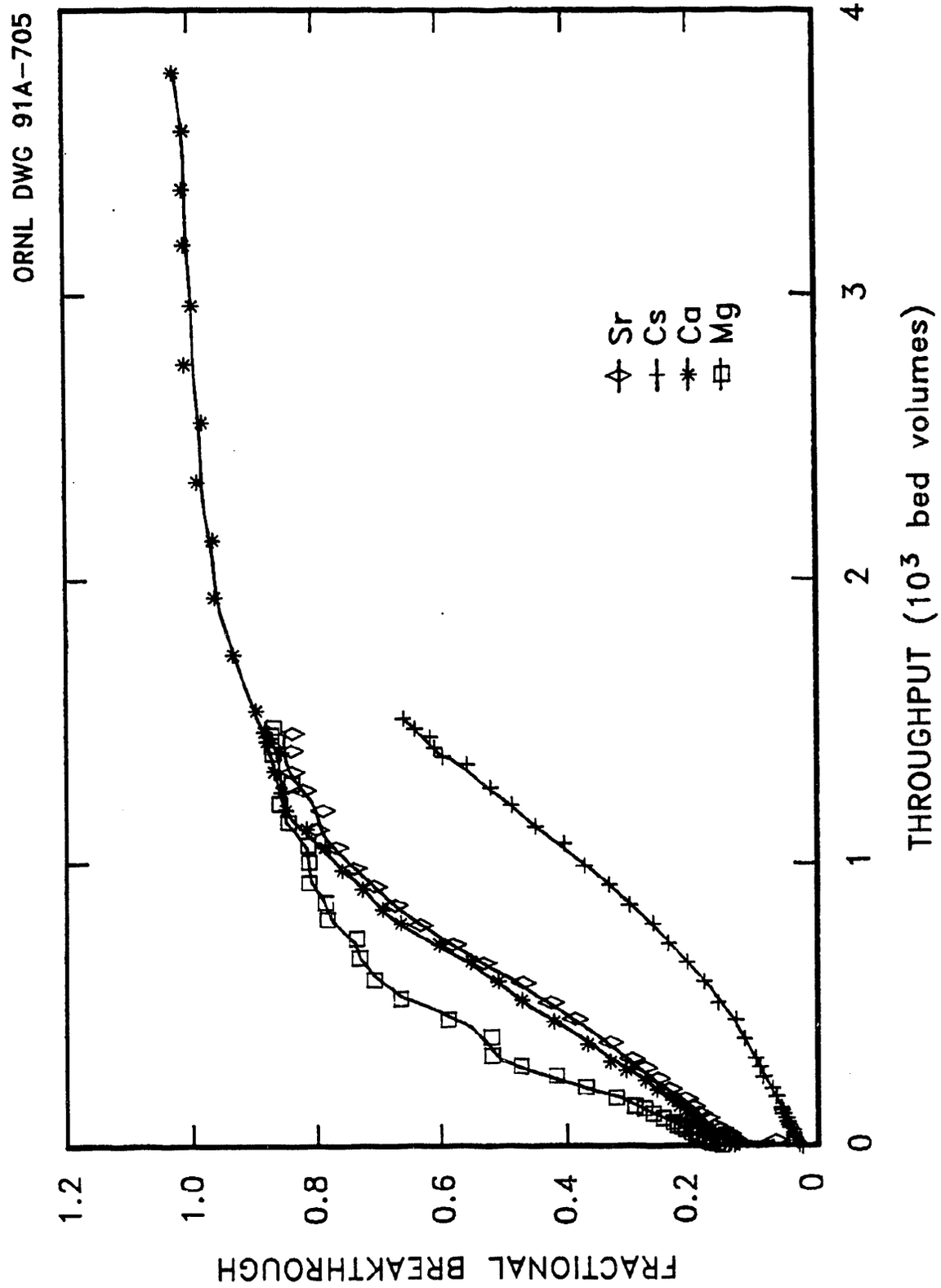

Figure 5a. Short-bed adsorber breakthrough curves in a single component systems

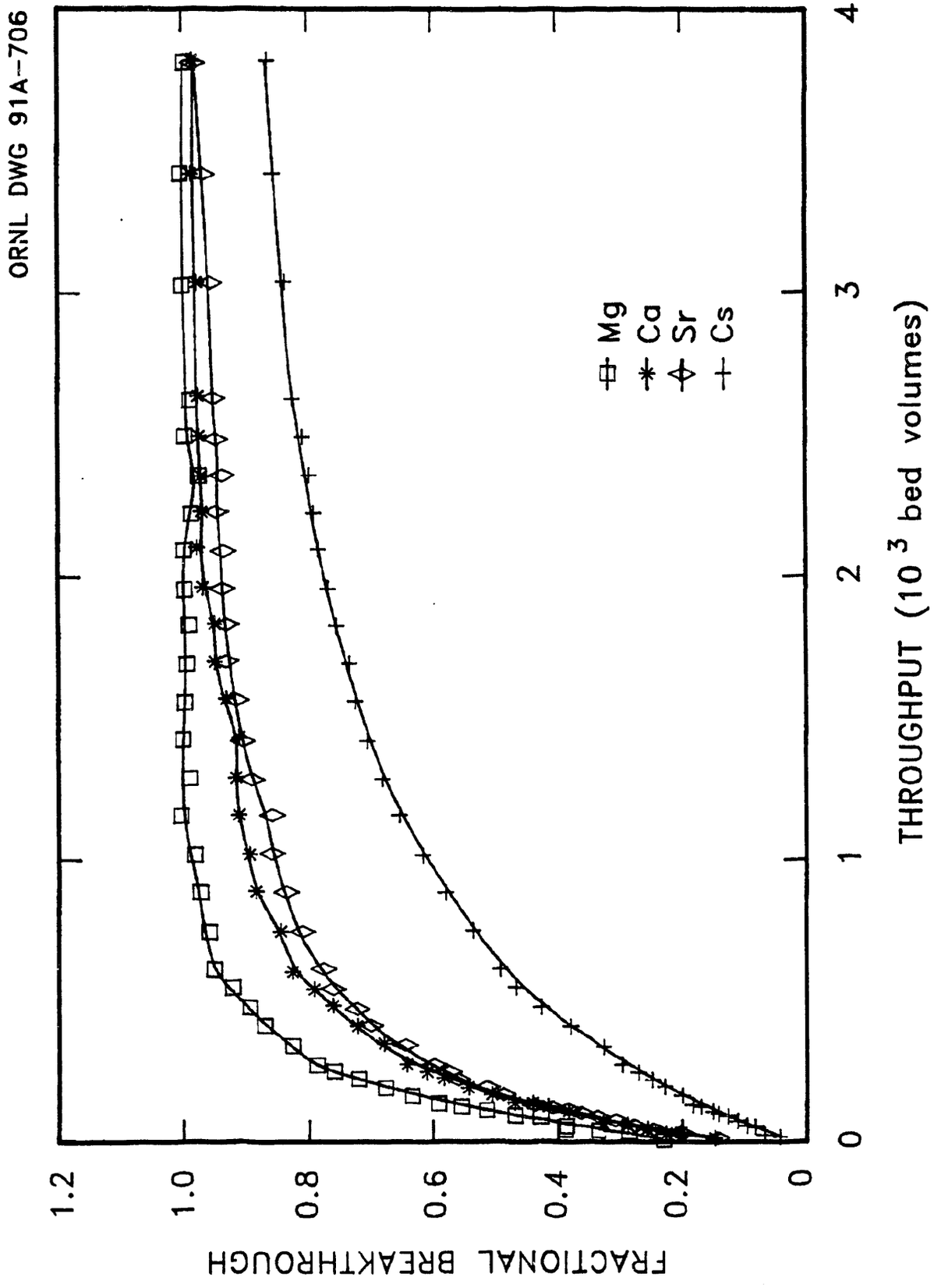

Figure 5b. Short-bed adsorber breakthrough curves in a multicomponent system.

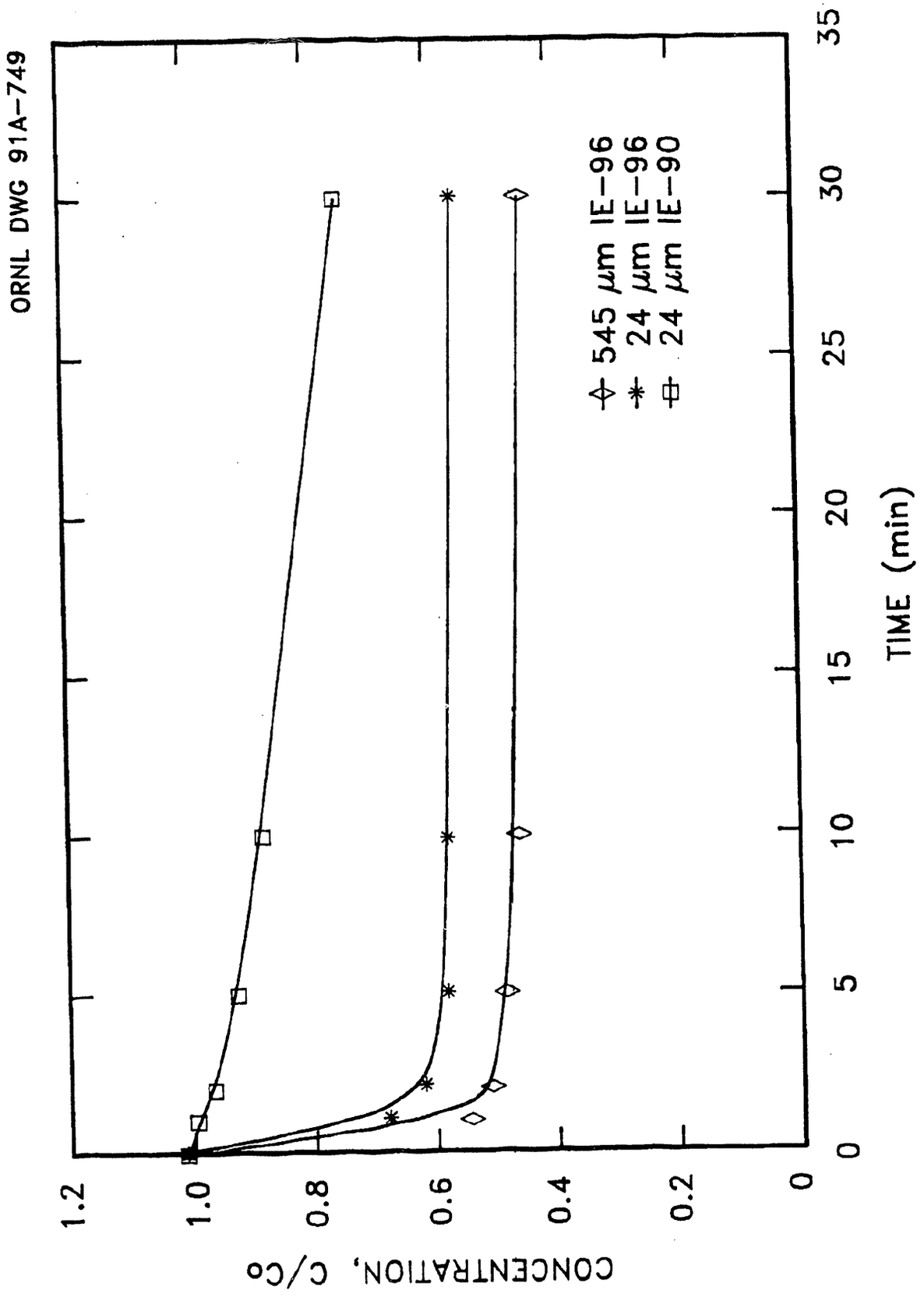

Figure 6a. Effect of particle size on uptake rate for a batch reactor using $CaCl_2$ feed in the solution phase.

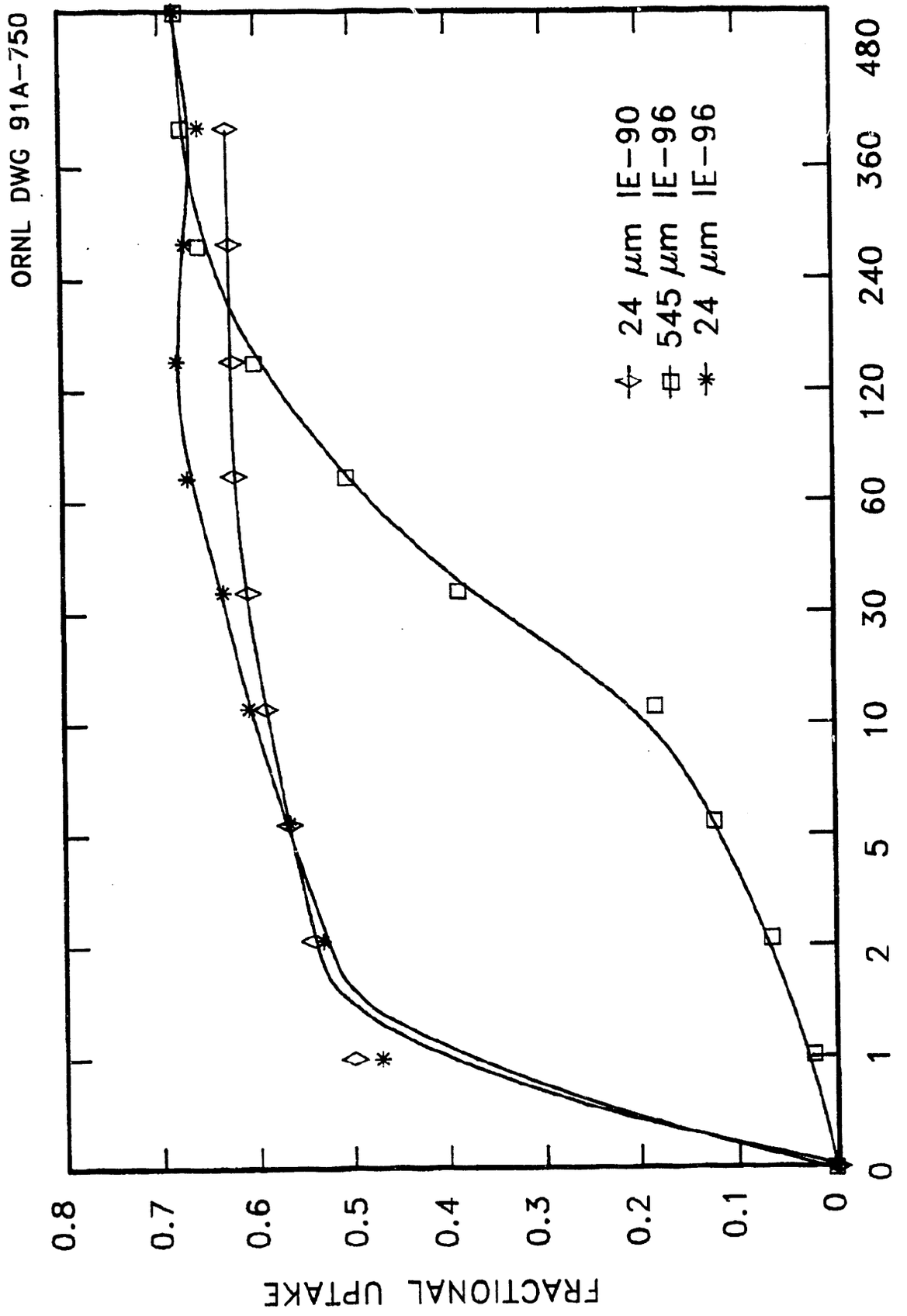

Figure 6b. Effect of particle size on uptake rate for a batch reactor using $CaCl_2$ feed in the solids phase.

Table 1. Parameters for isotherm equation

	Coefficients[a]			
Isotherm	b_0	b_1	b_2	R^2
Binary Systems				
Sr isotherm	-1.635	-0.6835	-0.05013	0.97
Cs isotherm	-2.165	-0.8850	-0.06261	0.95
Ca isotherm	1.827	0.2641	-0.00954	0.96
Mg isotherm	-0.465	-0.1279	-0.01202	0.74
Multicomponent System				
Sr isotherm	-4.742	-1.157	-0.07507	0.99
Cs isotherm	-1.532	-0.5890	-0.05002	0.99
Ca isotherm	-4.212	-0.8560	-0.04703	1.00
Mg isotherm	-17.28	-3.345	-0.1818	0.93

[a] See Equation 13.

Typical breakthrough curves for the SBA are shown in Figs. 3 - 5. Figure 3 shows the effect of flow rate on the initial portion of the breakthrough curves for 545-μm Ionsiv IE-96 with calcium chloride ($CaCl_2$) feed. Varying the flow rate from 3.2 to 11.6 mL/min significantly impacted the breakthrough curves, indicating that film mass transfer has a significant effect in these ranges. After approximately 2000 min, the curves converged indicating that film mass transfer has less of an effect after initial breakthrough. This is consistent with previous findings for the SBA (*4, 25, 26*).

Figure 4 shows the effect of varying the particle size of Ionsiv IE-96 at a flow-rate of 8.5 mL/min with $CaCl_2$ feed. Since the breakthrough curves are impacted by particle size, macropore intraparticle mass-transfer resistance is significant.

Figure 5 shows the single- and multicomponent breakthrough curves for 545-μm Ionsiv IE-96 at a flow rate of 8.5 mL/min. In all cases, the cation concentration at the initial breakthrough point was slightly higher for the multicomponent system, indicating that multicomponent interactions affect the film mass-transfer coefficients. The slopes of the breakthrough curves for all cations were also much steeper for the multicomponent system due to the interactive effects.

Figure 6 shows the calcium uptake curves for different particle sizes of Ionsiv IE-90 and IE-96 in a batch reactor. Since the curves were impacted by particle size, this confirms the trends seen in Fig. 4 which show that macropore mass-transfer resistance is significant. Since the uptake rates for IE-90 and IE-96 particles of the same size were not significantly different, micropore mass-transfer resistance is not limiting.

Film mass-transfer coefficients were estimated using the correlations given in Equations 16-26 and using Equation 27 for the SBA data for both binary and

multicomponent systems. Typical results for 545-μm particles are summarized in Table 2. The correlations predicted k_f values for the binary systems in the range of 0.001 to 0.008 cm/s with most ranging around 0.004 cm/s. Equation 27 predicted values from 0.004 to 0.009 cm/s for the binary systems. The correlations tended to underpredict k_f for binary data by factors up to 2, and the Williamson correlation (Equation 16) tended to agree best with Equation 27. Film mass-transfer coefficients calculated for multicomponent data were slightly lower than the corresponding values for binary systems. This trend is consistent with results seen in tests for removing organics from wastewaters using activated carbon *(32)*. Literature correlations for multicomponent systems are the same as those for binary systems since correlations do not account for solute interaction, the assumption being that solutes diffuse independently of one another. The relative magnitude of the values for k_f as a function of fluid flow rate and cation present were consistently predicted by the correlations and experimental data (both binary and multicomponent systems).

Film mass-transfer coefficients were estimated using the various correlations given in Equations 28-31 and Equation 32 for the batch reactor data. The k_f values were not a function of stirrer speed, and typical results are shown in Table 3. The correlations predicted k_f values in the range of 0.001 to 0.02 cm/s for 545-μm diam particles and 0.01 to 0.08 cm/s for 24-μm diam particles. The Treybal correlation predicted substantially lower values than the other equations for the larger particles, but resulted in similar predictions for 24-μm particles. Equation 32 predicted values from 0.01 to 0.09 cm/s for binary systems and 0.004 to 0.06 cm/s for the multicomponent system. This is consistent with the trend seen in column data. The experimental derived k_f values were a function of the cation present and particle size. The correlations tended to underpredict k_f by factors up

Table 2. Film mass-transfer coefficients for a column

Cation	Flow rate (mL/min)	k_f, cm/s									
		Williamson, et al. (Eq.16)	Wilson & Geankoplis (Eq.17)	Ohaski, et al. (Eq.18-20)	Gnielinsk (Eq. 21)	Katooka et al. (Eq. 23)	Dwivedi-μpadhyay (Eq. 24)	Ranz & Marshall (Eq. 25)	Wakas & Funaskii (Eq. 26)	Binary Data (Eq. 27)	Multicomponent Data (Eq. 27)
Ca	8.6	0.0047	0.0042	0.0037	0.0031	0.0036	0.0036	0.0028	0.0028	0.0067	0.0052
Sr	8.6	0.0047	0.0037	0.0035	0.0028	0.0033	0.0032	0.0026	0.0026	0.0071	0.0053
Mg	8.6	0.0045	0.0041	0.0035	0.0030	0.0035	0.0034	0.0026	0.0026	0.0042	0.0038
Cs	8.6	0.0052	0.0048	0.0043	0.0036	0.0041	0.0041	0.0032	0.0032	0.0086	0.0081
Ca	3.2	0.0035	0.0029	0.0026	0.0022	0.0026	0.0026	0.0018	0.0017	0.0039	-
Ca	11.6	0.0052	0.0047	0.0041	0.0032	0.0040	0.0040	0.0032	0.0032	0.0070	-

* Indicates not measured.

Table 3. Film mass-transfer coefficients for the batch reactor

Cation	Exchanger	Particle size, μm	k_f,cm/s					
			Treybal (Eq. 28)	Gilliland-Sherwood (Eq. 29)	Froessling (Eq. 30)	Sherwood, et al. (Eq. 31)	Binary data (Eq. 32)	Multicomponent data (Eq. 32)
Ca	IE-90	24	0.013	0.057	0.047	0.013	0.051	0.013
Sr	IE-90	24	0.013	0.057	0.047	0.013	0.071	0.060
Mg	IE-90	24	0.012	0.054	0.045	0.012	0.022	0.0041
Cs	IE-90	24	0.019	0.075	0.065	0.019	0.085	0.016
Ca	IE-96	545	0.0011	0.018	0.012	0.0090	0.021	0.0039
Sr	IE-96	545	0.0011	0.018	0.012	0.0090	0.018	0.0039
Mg	IE-96	545	0.0010	0.017	0.012	0.0086	0.010	0.0075
Cs	IE-96	545	0.0015	0.024	0.016	0.0120	0.026	0.0064

to 10, and the Gilliland-Sherwood correlation (Equation 29) agreed best with Equation 32 for the binary data. The relative magnitudes of the k_f values were consistently predicted as a function of particle size and cation present in the solution.

SUMMARY

This study has generated isotherm data for binary and multicomponent systems containing Ca, Mg, Na, Sr, and Cs for Ionsiv IE-96 zeolite. All data obtained in this study were accurately predicted by a Dubinin-Polyani-type model, but multicomponent data could not be predicted from binary data.

Film mass-transfer coefficients were estimated using various correlations and initial breakthrough data for both column and batch reactor. The experimentally derived film-transfer coefficients were on the order of 0.004 cm/s for the SBA and 0.02 cm/s for batch reactors containing 545-μm particles for binary systems. The values were a function of the cation present, the column flow rate, and the particle size. Literature correlations varied widely in their predictions of film mass-transfer coefficients and, in general, tended to underpredict experimentally derived values. Correlations were within a factor of 2 for predicting column coefficients, but were off as much as an order of magnitude for batch reactors.

Experimentally derived film mass-transfer coefficients for the multicomponent systems were lower than those obtained for the corresponding binary systems, indicating that

multicomponent interactions affect the film mass-transfer coefficients. Literature correlations do not predict multicomponent interactions.

The ORNL process waste treatment facility will be upgraded using a series of chabazite zeolite columns to remove ^{90}Sr and ^{137}Cs from wastewater. Bench-scale, pilot-scale, and near-full-scale tests indicated that standard scaleup techniques cannot be used to optimize the zeolite column design. Since the optimal operation of the ion-exchange columns is the key to the economic operation of this system, a predictive mathematical model is being developed for this purpose. This model will incorporate the effects of the equilibrium and mass-transfer mechanisms described in this paper on the column dynamics for multicomponent liquid ion exchange with zeolites. After verification in pilot tests, this model can be used to examine design parameters other than those directly measured and project column response and sensitivity to many variables. Because the model is based on the equilibrium and transport parameters of the system, it should also greatly reduce the need for future pilot-scale tests and reduce the uncertainty involved in the design of full-scale zeolite columns.

NOTATION

A equivalent fraction

a isotherm constant

b isotherm constant

c sorbate concentration, meq/mL

c_d bulk solution concentration, meq/mL

c_m solubility, meq/mL

c_0 initial solution concentration, meq/mL

c_p solution concentration at a particle surface, meq/mL

D_c micropore diffusivity, cm^2/s

d_i impeller diameter, cm

D_L liquid diffusivity, cm^2/s

D_p macropore diffusivity, cm^2/s

D_z axial dispersion coefficient, cm/s

d_t tank diameter, cm

ϵ bed void fraction

ϵ_p particle void fraction

g charge of cation

G acceleration due to gravity, cm/s^2

k isotherm constant

k_f film mass-transfer coefficient, cm/s

L column length, cm

m number of solutes

n exponent of the, Freundlich Isotherm

P specific power input, cm^2/s^3

$\bar{q}$ average concentration in solid phase, meq/g

q sorbent concentration, meq/g

q_c concentration is zeolite crystal, meq/g

q_s saturation limit, meq/g

R gas constant

Re $\dfrac{2\rho_L R_p \upsilon \epsilon}{\mu}$

r zeolite crystal radius, cm

Re_p $(2R_p)^{4/3} (pg_c/V_L)^{1/3} \rho_L^{2/3}/\mu$, where p is power in Nm/s.

ρ density of sorbent, g/cm^3

ρ_L density of liquid, g/cm^3

R_p particle radius, cm

Sc $\mu/\rho_L D_L$

Sh $2R_p k_f/D_L$

t time, sec

T temperature

V_L liquid volume, cm^3

z axial position in column, cm

υ fluid velocity, cm/s

μ viscosity, g/cm·s

Literature Cited

1. Sherman, J. D., AIChE Symp. Ser., *Ion-exchange Separations with Molecular Sieve Zeolites*, 1978, **74**, 179.
2. Robinson, S. M., and Parrott, Jr., J. R., *Pilot-Scale Demonstration of Process Wastewater Decontamination Using Chabazite Zeolites*, ORNL/TM-10836, Oak Ridge National Laboratory, Oak Ridge, TN, December 1989.
3. Robinson, S. M., et al., *The Development of a Zeolite System for Upgrade of the ORNL Process Waste Treatment Plant*, ORNL/TM-11426, Oak Ridge National Laboratory, Oak Ridge, TN, in publication.
4. Weber, Jr., W. J.; Smith, E. H.; "Simulation and Design Models for Adsorption Processes," *Environ. Sci. Technol.*, **21(11)**, 1987, 1040-50.
5. Wankat, P. C., *Large-Scale Adsorption and Chromatography*; Vol. 1, CRC Press, 1986.
6. Dyer, A; Keir, D. "Nuclear Waste Treatment by Zeolites," *Zeolites*, **4**, 1984, 215-217.
7. Liang, S.; Weber, W. J., Jr. "Parameter Evaluation for Modeling Multicomponent Mass Transfer, *Chem. Eng. Commun.*, **35**, 1985, 49-61.
8. Robinson, S. M.; Arnold, W. D.; Byers, C. H. "Design of Fixed-Bed Ion-Exchange Columns for Wastewater Treatment"; Deutsch, B. P., Ed; In *HAZTECH International '90 Conference Proceedings*, Houston, Texas, 1990, 807.
9. Robinson, S. M.; Arnold, W. D.; Byers, C. H. "Multicomponent Ion-Exchange Equilibria in Chabazite Zeolite"; In 1990 ACS Symposium Series No. 468, *Emerging Technologies in Hazardous Waste Management II*, American Chemical Society, Washington, DC, 1991.
10. Breck, D. W., *Zeolite Molecular Sieves*, Wiley and Sons, New York, 1974.
11. Ruthven, D. M., *Principles of Adsorption and Adsorption Processes*, John Wiley & Sons, New York, 1984.
12. Soldatov, V. S.; Bichkova, V. A. "Ion Exchange Selectivity and Activity Coefficients as Functions of Ion Exchange Composition," *Separ. Sci.*, **15**, 1980 89-110.
13. Myers, A. L.; Byington, S. "Thermodynamics of Ion-Exchange: Prediction of Multicomponent Equilibria from Binary Data," In *Ion-exchange: Science and Technology*, Rodrigues, A. E., Ed.; NATO ASI Series E 107; Martinus Nijhoff Publishers; Boston, 1986, 119-145.
14. Shallcross, D. C., Hermann, C. C., and McCoy, B. J. "An Improved Model for the Prediction of Multicomponent Ion Exchange Equilibria," *Chem. Eng. Sci.*, **43(2)**, 1988, 79-288.
15. Crittenden, J. C. et al. "Prediction of Multicomponent Adsorption Equilibria Using Ideal Adsorbed Solution Theory," *Environ. Sci. Technol.*, 1985, **19(11)**, 1037-43.
16. Teo, J. K.; Ruthven, D. M. "Adsorption of Water from Aqueous Ethanol Using 3-A Molecular Sieves," *Ind. Eng. Chem. Process Des. Dev.*, 1986, **25**, 17-21.
17. Williamson, J. E.; Bazaire, K. E.; Geankoplis, C. J., *Ind. and E. C. Fund.*, **2**, 1963, 126-9.
18. Wilson, E. J.; Geankoplis, C. J., *Ind. Eng. Chem. Fund.*, **5**, 1966, 9-12.
19. Ohashi, H., et al., *J. Chem. Eng. Japan*, **14**, 1981, 433-8.
20. Roberts, P. V.; Cornel, P.; Summers, R. S., *J. Environ. Eng.*, **1**, 1985, 891-905.

21. Katoaka, T.; Yoshida,H.; Ueyama, K. J., *Chem. Eng. Japan*, **5**, 1972, 132-6.
22. Dwivedi, P. N.; Upadhyay, S. N., *Ind. Eng. Chem. Proc. Des. and Dev.*, **16**, 1977, 157-65.
23. Ranz, W. E.; Marshall, W. R., *Chem. Eng. Prog.*, **48**, 1952, 173.
24. Wakao, N.; Funazkri, T., *Chem. Eng. Sci.*, **33**, 1978, 1375.
25. Liu, K. T.; Weber, W. J., Jr. "Characterization of Mass Transfer Parameters for Adsorber Modeling and Design," *Journal WPCF*, **53(10)**, 1981, 1541-50.
26. Weber, W. J., Jr.; Wang, C. K. "A Microscale System for Estimation of Model Parameters for Fixed-Bed Adsorbers"; *Environ. Sci. Technol.*, **21(11)**, 1987, 1086-1102.
27. Letterman, R. D.; Quon, J. E.; Gemmell, R. S. "Film Transport Coefficient in Agitated Suspensions of Activated Carbon," *Journal WPCF*, **46(11)**, 1974, 2536-2546.
28. Sherwood, T. K.; Pigford, R. L.; Wilke, C. R., *Mass Transfer*, McGraw-Hill, New York, 1975, 220-224.
29. Treybal, R. E. *Mass-Transfer Operations*, McGraw-Hill, New York, 1980, 603.
30. McKay, G.; Bino, M. J. "Adsorption of Pollutants from Wastewater onto Activated Carbon Based on External Mass Transfer and Pore Diffusion," *Wat. Res.*, **22(3)**, 1988, 279-286.
31. Furusawa, T.; Smith, J. M. "Fluid-Particle and Intraparticle Mass Transport Rates in Slurries," *Ind. Eng. Chem. Fundam.*, **12(2)**, 1973, 197-203.
32. Smith, E. H.; Weber, W. J., Jr. *Environ. Sci. Technol.*, **22(3)**, 1988, 313-21.

END

DATE FILMED

12/31/91